

8-9-1989

## Electron Beam Testing of Integrated Circuits Using a Picosecond Photoelectron Scanning Electron Microscope

Y. Pastol

*T.J. Watson Research Center*

J. -M. Halbout

*T.J. Watson Research Center*

P. May

*T.J. Watson Research Center*

G. Chiu

*T.J. Watson Research Center*

Follow this and additional works at: <https://digitalcommons.usu.edu/microscopy>



Part of the [Life Sciences Commons](#)

---

### Recommended Citation

Pastol, Y.; Halbout, J. -M.; May, P.; and Chiu, G. (1989) "Electron Beam Testing of Integrated Circuits Using a Picosecond Photoelectron Scanning Electron Microscope," *Scanning Microscopy*: Vol. 3 : No. 2 , Article 6.

Available at: <https://digitalcommons.usu.edu/microscopy/vol3/iss2/6>

This Article is brought to you for free and open access by the Western Dairy Center at DigitalCommons@USU. It has been accepted for inclusion in Scanning Microscopy by an authorized administrator of DigitalCommons@USU. For more information, please contact [digitalcommons@usu.edu](mailto:digitalcommons@usu.edu).



## ELECTRON BEAM TESTING OF INTEGRATED CIRCUITS USING A PICOSECOND PHOTOELECTRON SCANNING ELECTRON MICROSCOPE

Y. Pastol(\*), J.-M. Halbout, P. May, and G. Chiu

IBM Research Division, T.J. Watson Research Center  
P. O. Box 218, Yorktown Heights, NY 10598

(Received for publication April 10, 1989, and in revised form August 09, 1989)

### Abstract

A scanning electron microscope which uses an ultrashort pulsed laser / photocathode combination as an electron source produces electron pulses of about 1 ps in duration at a 100 MHz repetition rate. By using this instrument in the stroboscopic voltage contrast mode we have performed waveform measurements at the internal nodes of high speed silicon integrated circuits at room and at liquid nitrogen temperature, and studied the propagation of ultrafast electrical transients on various interconnection structures.

**Key Words:** Picosecond photoelectron pulses, high speed waveform measurements, electron beam testing of integrated circuits.

\*Address for correspondence:  
IBM T.J. Watson Research Center, P.O. Box 218,  
Yorktown Heights, NY 10598, USA. Phone No (914) 945  
3284

### Introduction

The constant advances in integrated circuit technology leads to ever faster devices with ever smaller dimensions. For example, silicon NMOS circuits with 0.1  $\mu\text{m}$  gate length have recently achieved 13.1 ps gate delay (Sai-Halasz et al., 1988). Clearly, picosecond temporal resolution and submicron spatial resolution are needed to characterize the performance of such high speed circuits. This has stimulated much recent work on contactless techniques for ultrafast electrical waveform measurements. Many of these approaches use a laser-generated optical probe (Kolner and Bloom, 1986, Weingarten et al., 1988, Bokor et al., 1986, Marcus et al., 1986, Blacha et al., 1987, Heinrich et al., 1986), and take advantage of the high temporal resolution readily available with pulsed lasers. However, because of their inherent limits in spatial resolution, these all-optical techniques are likely to encounter difficulties as electronic devices and wiring are scaled down to submicron dimensions.

Electron beam testers, i.e., scanning electron microscopes (SEMs) operated in the stroboscopic voltage contrast mode have also been developed (For an in-depth review of the field, see for example: Feuerbaum, 1983, Menzel and Kubalek, 1983a). They conventionally rely on fast deflection beam blanking systems to create the electron probe pulses (Menzel and Kubalek, 1979), sometimes even associated with a bunching mode of operation (Hosokawa, 1978). One drawback of these blanking systems is that they impose small average beam current and therefore long measurement times to recover waveforms with good signal to noise ratio. Another disadvantage is that, at the beam energies suitable for probing integrated circuits, typically 0.7 to 2 keV, there is detrimental spot size degradation and submicron spatial resolution is difficult to achieve simultaneously with high temporal resolution. Commercial electron beam testers have achieved 100 ps risetime/falltime resolution with 10 ps jitter (Todokoro et al., 1986) and it is therefore essential to advance the already well established electron beam probing technology into the picosecond regime.

We recently developed an ultrafast electron beam probe called the picosecond photoelectron scanning electron microscope (PPSEM) (May et al., 1987, May et al., 1988, Halbout et al., 1988a,b) which combines the high temporal resolution of the laser techniques and the high spatial resolution of the SEM. This instrument is used for noncontact internal waveform measurements on high speed integrated circuits, and for studying the propagation of ultrafast electrical transients on various interconnection structures.

### Description of the instrument

In the PPSEM, the thermionic electron gun of a conventional SEM has been replaced by a pulsed laser/photocathode combination (see Fig. 1). The source of optical pulses is a mode-locked, pulse-compressed and frequency-doubled Nd:YAG laser. Its 532 nm wavelength output consists of pulses of 2 ps duration at a 100 MHz repetition rate and 300 mW average power. Subsequent frequency doubling in a KDP crystal yields over 3 mW of average ultraviolet (u.v.) power at 266 nm with 1.5 ps pulses. The u.v. light is focussed onto a photocathode mounted at the head of the SEM column. This photocathode consists of a roughened gold film of 20 nm thickness evaporated on a fused silica substrate, and is used in transmission with the light focussed through the transparent substrate. The photoelectrons are produced by single photon photoemission with approximately 6000 electrons in each 1.5 ps pulse. The peak brightness of this pulsed electron source is  $3.10^8$  A/cm<sup>2</sup>steradian at an accelerating voltage of 1.8 keV, which is comparable to the field emission regime (Wells, 1974, Orloff, 1984) without, however, the high vacuum requirements: the photoelectron gun vacuum is typically  $1.33 \cdot 10^{-4}$  Pa during operation. Under these conditions, the cathode lifetime is several hundred hours.

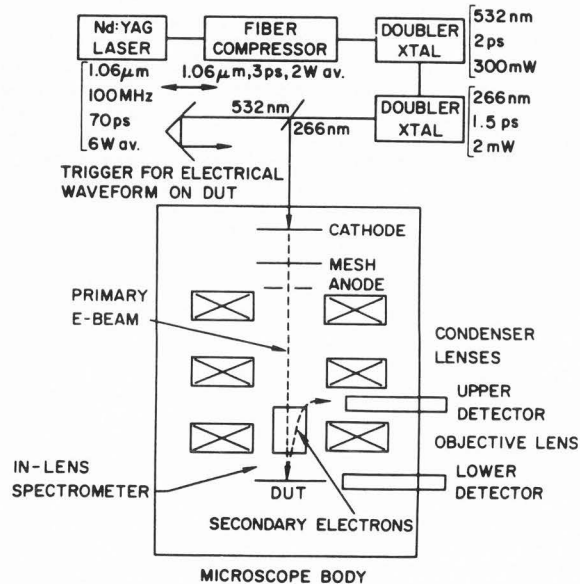


Figure 1. Schematic of the picosecond photoelectron SEM.

Since the spot size on the photocathode is relatively small ( $4 \mu\text{m}$ , i.e., comparable with the beam diameter at its crossover point in a thermionic gun), it can be used directly as the object for the electron optics without the need for a Wehnelt electrode. A high extraction field at the photocathode minimizes the pulse broadening due to Coulomb interactions and also raises the threshold for the onset of space-charge effects (Massey, 1984). This can be accomplished either with a mesh or an aperture in close proximity with the cathode, or by reducing the cathode-anode spacing. We typically operate at accelerating fields between 1 and 1.5 kV/mm. Most of the voltage drop occurs between the cathode and the extraction mesh when such a configuration is used. Measurements show that the emitted photocurrent follows the u.v. average power linearly, which clearly indicates that we are not operating in the space-charge limited regime.

The primary electron beam thus produced is focussed

on the circuit under test using the electron optics of the SEM. The typical average sample current is 50 pA for an average cathode current of 10 nA. A picture of the area of interest is then obtained at the desired magnification in the conventional way, by raster scanning the pulsed electron beam and displaying the image corresponding to the time-integrated secondary electron current. For voltage measurements, an in-lens three grids planar energy analyzer, based on a simplified Feuerbaum design (Feuerbaum, 1979, Menzel and Kubalek, 1983b), was implemented. Extraction fields between 0.5 and 1 kV/mm are used during the measurements. The circuit or device under test is exercised in synchronism with the train of optical pulses, and the waveforms are reconstructed by an equivalent time sampling technique which consists in progressively delaying the ultrashort probe electron pulse with respect to the circuit trigger. Usual waveform recording times are of the order of 20 seconds. As presented earlier (May et al., 1987), the PPSEM has demonstrated a 5 ps temporal resolution, a spatial resolution of  $0.1 \mu\text{m}$ , both in terms of probe size and probe placement, and a voltage sensitivity of  $3 \text{ mV}/(\text{Hz})^{1/2}$ .

### Measurements on circuits

#### Passive interconnects

In our first example of application of this tool, we present measurements on an experimental interconnection structure fabricated with a thin-film technology (Arjavalingam et al., 1988). The sample under investigation consists of a series of  $8 \mu\text{m}$  wide and  $5.35 \mu\text{m}$  thick copper microstrip transmission lines separated from a uniform ground plane by a  $6.5 \mu\text{m}$  thick layer of polyimide (Fig. 2a). The lines are embedded in the polyimide, with only their top surface exposed. The line spacing is  $25 \mu\text{m}$  from center to center. Electrical pulses, 100 ps in duration, produced by a step-recovery diode were launched on one of these transmission lines by means of a high bandwidth short coaxial cable (Halbout et al., 1988a). Measurements were made at the beginning and also at several points along the line (Figs. 2b and 2c). The first peak in the recorded waveform corresponds to the input pulse travelling past the measurement point. The second peak corresponds to the same pulse reflected back from the end of the 25 mm long open-circuited line. From the attenuation and broadening of this second pulse it is possible to determine the characteristic loss and dispersion of the transmission line.

#### $0.5 \mu\text{m}$ CMOS SRAM

As a second example, we present room temperature and low temperature ( $80^\circ\text{K}$ ) measurements of the access time of a  $0.5 \mu\text{m}$  CMOS SRAM from the clock input to the cell, and its breakdown into individual delays between logic devices (inverters, NOR and NAND gates) in the prelogic leading to the selected cell (Halbout et al., 1988b, Pastol et al., 1988). The circuit was fabricated in a  $0.5 \mu\text{m}$  selectively scaled CMOS technology (Wang et al., 1986). The smallest dimension at the metal level is  $1.2 \mu\text{m}$  line width with  $1.0 \mu\text{m}$  contacts. To synchronize the measured waveforms to the pulsed electron probe, a photodiode is used to provide the trigger to a pulse generator that in turn supplies a 100 MHz square wave signal (3.3 V amplitude) to the clock pad on the chip. A particular memory cell in this experimental 576 bit SRAM is selected by supplying appropriate static address voltages. The chip was mounted in a 40 pin dip package and placed on the x-y stage of the PPSEM. The package can be cooled down to  $80^\circ\text{K}$  (measured with a diode) by a liquid nitrogen flow; this permits low temperature measurements. The logic path from the clock input to the cell is shown in Fig. 3a where the measurement points are identified by numbers. Figure 3b shows the room temperature and low temperature measured

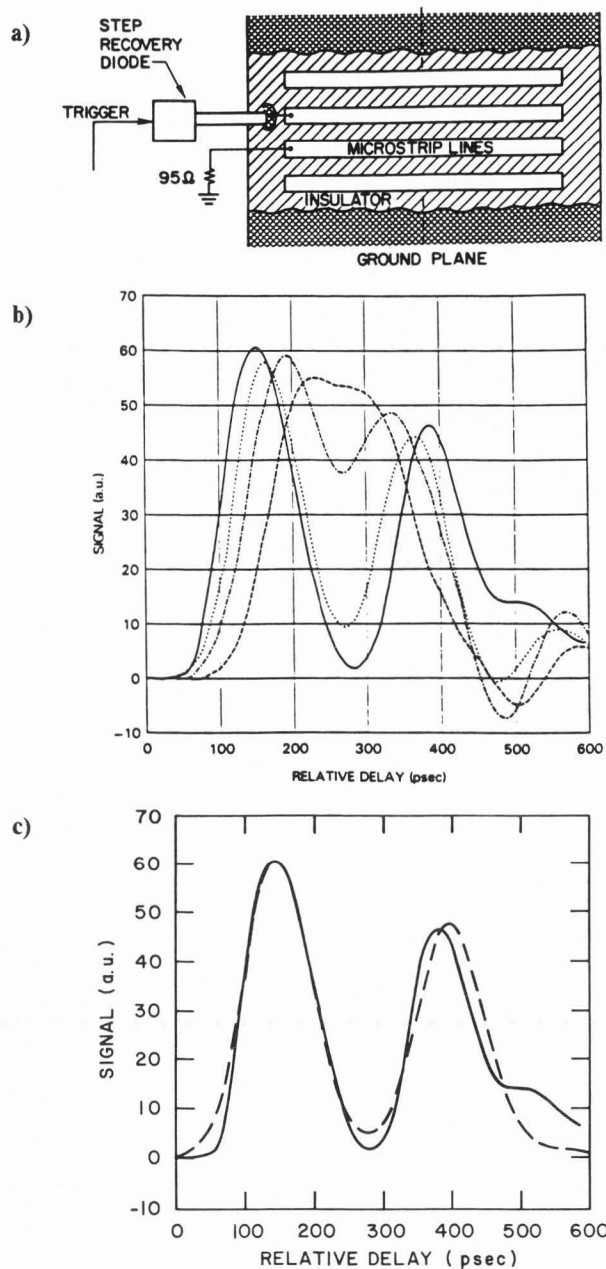


**Figure 2.** (a) Schematic of the experimental thin-film interconnection structure. (b) Waveforms measured at various points along a thin-film microstrip transmission line. 0 mm, solid line; 5 mm, dotted line; 10 mm, dotted dash line; 15 mm, dashed line. (c) Comparison between the 0 mm data and a simulation.

waveforms. The overall access time to the cell is 1400 ps at room temperature, and 1110 ps at 80 °K. With the high temporal resolution of the apparatus, it is possible to characterize each logic gate in terms of risetime/falltime and gate delay, and to accurately determine how these characteristics are modified at low temperature. We also measured, at room temperature, a 40 ps on-chip wiring delay between the two extremities of a 500 μm long line (Fig. 4). This is, to the best of our knowledge, the first accurate

measurement of an on-chip wiring delay.

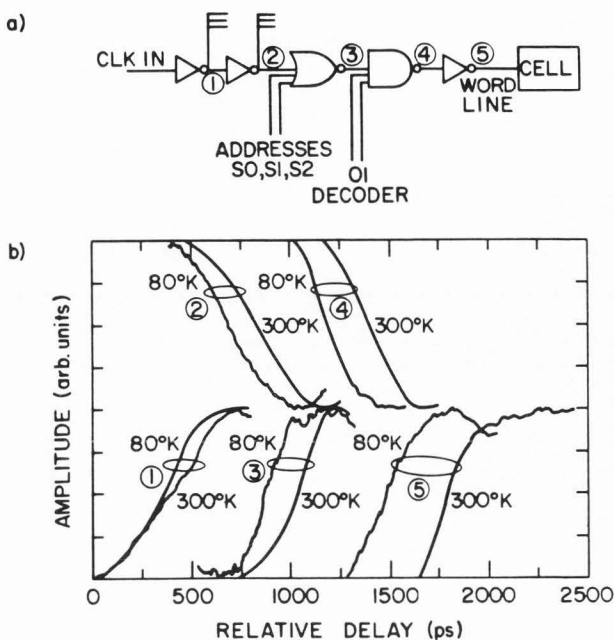


**Figure 3.** (a) Schematic of the device path from the clock input to the cell. (b) Room temperature and low temperature waveforms from the first inverter to the memory cell. Note that the dc levels have been shifted for easy timing comparison: falling edges are depicted in the top half, rising edges in the bottom half. The overall access time is measured between waveforms 1 and 5 at 50 % of the total voltage swing.

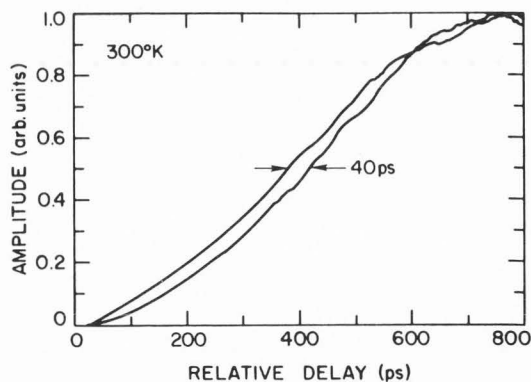


**Figure 4.** On-chip propagation delay measured between the two extremities of a 500 μm long interconnection line.

#### 0.25 μm gatlength inverter chain

Finally, inverter chains fabricated in a 0.25 μm gatlength silicon NMOS technology (Sai-Halasz et al., 1987) were also investigated at room temperature. The circuits are externally triggered by a photodiode-pulse generator combination, as described above. The measurements are performed by directing the pulsed electron probe on the 0.25 μm wide lines interconnecting the successive stages of the chain. The corresponding results are displayed in Fig. 5 for the output of four consecutive inverters inside the

chain. An average gate delay of 23 ps, and risetimes/falltimes of 25 ps are observed for room temperature operation. These measurements clearly demonstrate the simultaneous temporal and spatial resolutions of the PPSEM.

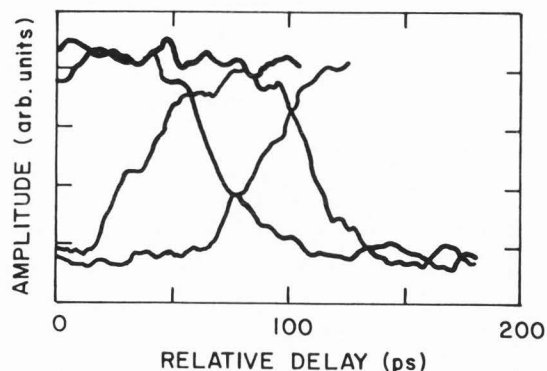


**Figure 5.** Output waveforms of four consecutive stages in a  $0.25 \mu\text{m}$  NMOS inverter chain. From left to right, outputs of the 1st inverter (1st rising edge), 2nd inverter (1st falling edge), 3rd inverter (2nd rising edge), and 4th inverter (2nd falling edge).

### Conclusion

A laser-pulsed SEM, the picosecond photoelectron scanning electron microscope has been developed, and has demonstrated a 5 ps temporal resolution, a probe size of  $0.1 \mu\text{m}$ , and a voltage resolution of  $3 \text{ mV}/(\text{Hz})^{1/2}$ . This instrument has been used for measuring high speed electrical waveforms on integrated circuits with a temporal accuracy so far unsurpassed by electron beam testers. More recently, a feedback circuitry was combined with the in-lens spectrometer (Fentem and Gopinath, 1974) to permit quantitative voltage contrast operation. A computerized image processing capability has also been implemented. This shows that the sophisticated technology of electron beam testing can be directly adapted to the PPSEM with, for instance, workstation environment allowing access to the circuit CAD data files during a test sequence (Concina and Richardson, 1987).

### References

- Arjavalingam G, May P, Halbout J-M, Kopcsay GV (1988). Characterization of an experimental thin-film interconnection structure. *SPIE Proceedings* 947, 131-137.
- Blacha A, Clauberg R, Seitz HK, Beha H (1987). 17 ps rise-time measurement by photoemission sampling. *Electron Lett* 23, 249-250.
- Bokor J, Johnson AM, Storz RH, Simpson WM (1986). High speed circuit measurements using photoemission sampling. *Appl Phys Lett* 49, 226-228.
- Concina S, Richardson N (1987). Workstation-driven e-beam prober. *International Test Conference 1987 Proceedings*, 554-560, published by the Institute of Electrical and Electronics Engineers, Inc. (IEEE), 345 E. 47th St., New York, NY 10017, USA.
- Fentem PJ, Gopinath A (1974). Voltage contrast linearization with a hemispherical retarding analyzer. *J Phys E: Scientific Instruments* 7, 930-933.
- Feuerbaum HP (1983). Electron beam testing: methods and applications. *Scanning* 5, 14-24.
- Feuerbaum HP (1979). VLSI testing using the electron probe. *Scanning Electron Microsc.* 1979; I: 285-296.
- Halbout JM, May P, Chiu G (1988a). Ultrashort electron pulse probing of integrated circuits. *J Mod Optics* 35, 1995-2005.
- Halbout JM, May P, Jenkins K, Compeau G (1988b). SRAM access time measurement using a picosecond photoelectron scanning electron microscope. *ISSCC Tech Dig*, 82-84, published by the Institute of Electrical and Electronics Engineers, Inc. (IEEE), 345 E. 47th St., New York, NY 10017, USA.
- Heinrich HK, Bloom DM, Hemenway BR (1986). Noninvasive sheet charge density probe for integrated silicon devices. *Appl Phys Lett* 48, 1066-1068.
- Hosokawa T, Fujioka H, Ura K (1978). Gigahertz stroboscopy with the scanning electron microscope. *Rev Sci Instrum* 49, 1293-1299.
- Kolner BH, Bloom DM (1986). Electrooptic sampling in GaAs integrated circuits. *IEEE J Quantum Electron* QE-22, 79-93.
- Marcus RB, Weiner AM, Abeles JH, Lin PSD (1986). High speed electrical sampling by fs photoemission. *Appl Phys Lett* 49, 357-359.
- Massey GA (1984). Laser photoelectron source of high apparent brightness. *IEEE J Quantum Electron* QE-20, 103-105.
- May P, Halbout JM, Chiu G (1987). Picosecond photoelectron scanning electron microscope for noncontact testing of integrated circuits. *Appl Phys Lett* 51, 145-147.
- May P, Halbout JM, Chiu G (1988). Noncontact high speed waveform measurements with the picosecond photoelectron scanning electron microscope. *IEEE J Quantum Electron* 24, 234-239.
- Menzel E, Kubalek E (1979). Electron beam chopping systems in the SEM. *Scanning Electron Microsc.* 1979; I: 305-318.
- Menzel E, Kubalek E (1983a). Fundamentals of electron beam testing of integrated circuits. *Scanning* 5, 103-122.
- Menzel E, Kubalek E (1983b). Secondary electron detection systems for quantitative voltage measurements. *Scanning* 5, 151-171.
- Orloff J (1984). A comparison of electron guns for high speed electron beam inspection. *Scanning Electron Microsc.* 1984; IV: 1585-1600.
- Pastol Y, Halbout JM, May P, Compeau G (1988). Noncontact internal waveform measurements with picosecond time resolution on a  $0.5 \mu\text{m}$  CMOS SRAM. *IEEE Electron Device Lett* 9, 506-508.
- Sai-Halasz GA, Wordeman MR, Kern DP, Ganin E, Rishton S, Ng HY, Moy D, Chang THP, Dennard RH (1988). Inverter performance of deep submicron MOSFETs. *IEEE Electron Device Lett* 9, 633-635.
- Sai-Halasz GA, Wordeman MR, Kern DP, Rishton S, Ganin E (1987). Experimental technology and characterization of self-aligned  $0.1 \mu\text{m}$ -gate length low-temperature operation NMOS devices. *IEDM Tech Dig* 397-400, published by the Institute of Electrical and Electronics Engineers, Inc. (IEEE), 345 E. 47th St., New York, NY 10017, USA.
- Todokoro H, Yoneda S, Seitou S, Hosoki S (1986). Electron beam tester with 10 ps time resolution. *ITC Tech Dig* 600-606, published by the Institute of Electrical and Electronics Engineers, Inc. (IEEE), 345 E. 47th St., New York, NY 10017, USA.
- Wang LK, Taur Y, Moy D, Dennard RH, Chiong K, Hohn F, Coane PJ, Edenfeld A, Carbaugh S, Kenney D, Schnur S (1986).  $0.5 \mu\text{m}$  gate CMOS technology using e-beam/optical mix lithography. *Symposium on VLSI*

Technology, Dig. Tech. Papers, 13-14, published by the Institute of Electrical and Electronics Engineers, Inc. (IEEE), 345 E. 47th St., New York, NY 10017, USA.

Weingarten KJ, Rodwell MJW, Bloom DM (1988). Picosecond optical sampling of GaAs integrated circuits. *IEEE J Quantum Electron* 24, 198-220.

Wells OC (1974). *Scanning Electron Microscopy*. McGraw Hill, New-York, 97-98.

### Discussion with Reviewers

H. Fujioka: Would you please comment on the short term (per minute) and long term (per hour) stabilities in the probe beam current?

Authors: The short term stability of the probe beam current is determined essentially by the laser power stability. After several hours of continuous operation, hydrocarbon contamination on the photocathode can cause a slow decrease of the electron beam current. This problem was solved by using a separate ion pumping system for the photoelectron gun.

H. Fujioka: Is it easy to change the repetition rate of the pulsed electron beam from 100 MHz to other frequencies, for example to 1 MHz or 1 GHz?

Authors: The system as described here can readily test circuits at multiples of the laser repetition rate, well into the GHz clocking regime by phase-locking a high frequency synthesizer to the laser frequency. By pulse picking, it is also possible to obtain sampling rates which are subharmonics of the laser repetition rate, and therefore test circuits at subharmonics of the 100 MHz frequency.

H. Fujioka: What type of delay circuit is used in your experimental system?

Authors: We use an optical variable delay line consisting of a retroreflector mounted on a translation stage driven by a stepper motor (0.04 ps/step).

P. Girard: Basing on your results, the system is now operating below the Coulomb effects range, do you think that a significant improvement of the photoemission yield or pulse power would be of interest in your equipment?

Authors: We recently replaced the KDP doubling crystal with an ADP crystal, which has a much higher u.v. conversion efficiency. We now obtain 5 mW average u.v. power and a typical cathode current of 20 nA. This results in an improved signal to noise ratio for both image formation and waveform measurements.

P. Girard: Have you encountered any serious problems related to transit time effects on secondary electrons? Could you describe the PPSEM possibilities or limits for the examination of passivated devices?

Authors: The temporal resolution of the instrument is very dependent both on the extraction field used and on the geometry of circuit under test, as both determine the time spent by secondary electrons under the influence of local fields above the sample. For lines with 5  $\mu\text{m}$  separation, we observed that the temporal resolution improves with increasing extraction field but that this improvement levels off for extraction fields higher than 2 kV/mm. This was confirmed by Monte-Carlo simulations. For passivated devices, we found that the energy of the primary electrons was very critical in obtaining reproducible results. Only when the primary beam energy was close to the upper unity yield point could we trust the waveform measurements. Under these conditions, accurate timing information can be obtained.

L. Balk: As the electron beam is probably not ideally monochromatic in its energy, the pulse generated at the cathode may broaden during its propagation. Can you comment on the pulse deterioration due to this effect? Especially, it would be interesting, if you have measured the pulse waveform at the sample position.

Authors: The temporal broadening of the electron probe pulse as it travels down the column chiefly arises from Coulomb repulsion between electrons. This longitudinal Boersch effect occurs mainly close to the photocathode, before the electrons have been fully accelerated, and to a lesser extent at the foci of the electron optics. For the operating conditions of our instrument, Monte Carlo calculations of electrons in the cathode-mesh region show that this temporal broadening is likely to be about 1 ps. We did not measure directly the electron pulse waveform at the sample position (see discussion of the temporal resolution below).

L. Balk: The temporal resolution is affected by the jitter produced by the photodiode-pulse generator combination. Can you give an estimation for the value of this jitter?

Authors: The triggering jitter of the pulse generator degrades the time resolution for delay measurements to about 10 ps.

L. Balk: How is the time resolution defined in your experiments? Do you take into account the reduction in the temporal resolution due to secondary effects such as the influence of varying microfields on secondary electrons? Is the resolution value triple (probe size, temporal, voltage) as mentioned in the conclusions achievable simultaneously?

Authors: The reported 5 ps temporal resolution is indeed global and takes into account the broadening of the electron pulse due to non-monochromaticity and Coulomb interactions as well as the influence of local fields above the sample. It was determined experimentally by measuring the temporal profile of electrical pulses photoconductively launched on 2.4  $\mu\text{m}$  coplanar aluminum transmission lines fabricated on a silicon on sapphire substrate, and comparing the measured risetime to that obtained on the same structure by photoconductive sampling, a high speed measurement technique with known temporal resolution. As stated in the conclusion, the temporal, spatial and voltage resolutions are achieved simultaneously.

A. Gopinath: The estimated width of the laser pulse is 1.5 ps, but the claimed temporal resolution is of the order of 5 ps. Could the authors explain the reasons for the difference?

Authors: The difference comes from the temporal broadening of the electron pulse as it travels down the column, and the influence of local fields above the circuit under test. Please see our answers to P. Girard and L. Balk for more details.

A. Gopinath: When the electron beam is generated by photoemission, it still remains a pulsed beam. What are the advantages compared to the pulsed beam generated by chopping across an aperture? Admittedly, the source is brighter and chopping degradation is eliminated.

Authors: The great advantage of the photocathode is its ability to produce a pulsed electron beam with a high peak brightness at low accelerating voltage, and free of chopping-related distortions.